ZIBELINE INTERNATIONAL™ PUBLISHING

ISSN: 2637-0778 (Online)
CODEN: ECRNAE

Environmental Contaminants Reviews (ECR)

DOI: http://doi.org/10.26480/ecr.02.2023.105.115

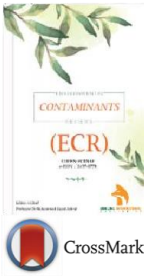

RESEARCH ARTICLE

ANALYSIS OF AEROSOLS IN WEST AFRICA: MODELLING AND RADIATIVE FORCING

Sharafa S.B.[a*], Aliyu R.[b], Ibrahim B.B.[c], Akpootu D.O.[a], Tijjani B.I.[d], Darma T.H.[d], Ayedun F.[e] and Sulu H.T.[f]

[a] Department of Physics, Usmanu Danfodiyo University Sokoto, Sokoto, Nigeria.
[b] Physics Department, Kano State University of Science and Technology Wudil, Kano, Nigeria.
[c] Physics/Electronics Unit, Kwara State Polytechnic, Ilorin, Nigeria.
[d] Physics Department, Bayero University Kano, Kano, Nigeria.
[e] Department of Pure and Applied Science, National Open University of Nigeria.
[f] Physics/Electronics Unit, Umaru Ali Shinkafi Polytechnic, Sokoto, Nigeria.
**Corresponding author email: sb69010@gmail.com; sharafa.salihu@udusok.edu.ng*

ARTICLE DETAILS

Article History:

Received 19 July 2023
Revised 22 August 2023
Accepted 25 September 2023
Available online 04 October 2023

ABSTRACT

We studied the aerosol properties in Cinzana and Ilorin in West Africa using data of aerosols' properties over the period 2000–2015 from MODIS (Moderate resolution Imaging Spectroradiometer). There has been limited report on the comparison between this two West African Stations. The time series modelling, prediction of aerosol parameters and the estimation of aerosol radiative forcing (ARF) were focused on. Statistical Package for the Social Sciences (SPSS) software was used for the modelling the monthly averaged measurements of aerosol optical depth at 550 nm (τ_{550}), Angstrom exponent at 470 – 660 nm ($\alpha_{470\text{-}660}$), cloud fraction (N_{cloud}), fine mode fraction (FMF) and single scattering albedo at 470 nm (ω_o) data over the two stations while the ARF values were calculated. The generated time series models are all good fit and the values are biased, both negatively and positively. The ARF of the two stations' aerosol data shows value between 0.0 and -750.0 W/m^2 for Ilorin and -10.0 to -200. 0 W/m^2, which results mainly in cooling. Although there is a difference between ARF values in the two stations, both stations demonstrated clear seasonal variation with the rainy season having the least negative aerosol forcing. The results suggest that the aerosols are predominantly mineral dust, but those in Cinzana have more absorbing properties than those in Ilorin. Overall, the research shows that the modelled parameters can be utilized in lieu of the measured data and that the solar radiation received in this region has been attenuated at various degrees.

KEYWORDS

EOT, Aerosols, Cinzana, Ilorin, Modelling, ARF

1. INTRODUCTION

Atmospheric aerosols are an inevitable issue in Atmospheric Physics and Chemistry (Kalluri, 2016). They are suspensions, in air, of solid or liquid particles, which are mostly observed as dust, smoke and haze. Their size ranges from a few nanometers to tens of micrometers. Although they make up a small fraction of the atmosphere, they are part of the key climate forcing agents recognized globally (Zhang and Reid, 2010; Annex III: Glossary In: Climate Change, 2013). They influence climate directly by scattering and absorbing solar radiation; thereby changing radiation budget at the top, bottom and within the atmosphere which in turn affect the atmospheric heating rate (Charlson, 1992). Absorbing aerosol (fine mode) particles can also heat the surrounding air, which can lead to evaporation of cloud droplets. It also has the ability to act as cloud condensation nuclei (CCN). This cloud effect is usually divided into two parts: the cloud albedo effect (an increase in aerosol concentrations leads to an increase in cloud droplets, which increases the albedo) and the cloud lifetime effect (increase in aerosol concentrations leads to smaller droplets, which reduces precipitation efficiency and prolong the cloud lifetime) thereby indirectly affecting terrestrial radiation (Ramanathan et al., 2001). Aerosols have also been found to have detrimental effects on human health, air quality and visibility (Zheng, 2016).

In spite of all the progress made in understanding atmospheric aerosols and their climatic effects, aerosol radiative forcing (ARF) is still characterized with lots of uncertainties in the analysis of climate change (Annex III: Glossary In: Climate Change, 2013; Patel et al., 2017; Bibi et al., 2017). This is, in part, because of the deficient knowledge of aerosol's spatio-temporal variability and their related properties (Alam et al., 2011; Kumar, 2014; Kumar, 2015; Boiyo et al., 2017). A sound knowledge of aerosols spatio-temporal variability as related to quantity, optical, microphysical and radiative properties is required to enrich our scientific understanding of their sources (natural and anthropogenic) and sinks, and to also give acceptable information to policy makers (Zhang and Reid, 2010). Because of these, different measurement ways have been put in place to monitor aerosols over different parts of the world (Kinne, 2003; Holben, 1998; Remer, 2005). Ground-based remote sensing network such as Aerosol Robotic Network (AERONET) and other Remote Sensing Network provides continuous datasets at multiple wavelengths to describe aerosol optical, microphysical and radiative properties (Alam et al., 2011).

Many studies using such networks have been reported in various parts of the globe (Zheng, 2016; Patel et al., 2017; Bibi et al., 2017; Alam et al., 2011; More et al., 2013; Adesina et al., 2014; Adesina et al., 2016; Kang et al., 2016; Bibi et al., 2016). Using ground-based AERONET data over Delhi (India), a group researchers reported change in ARF from 21.2 Wm^{-2} to 56.6 Wm^{-2} for clean and polluted environments, respectively (Kumar et al., 2016). Studies by some researchers at Karachi and Lahore (Pakistan) reported significant seasonal heterogeneity in ARF attributed to seasonal cycles of emission sources and meteorological variables (Alam et al., 2012; Bibi et al., 2017; Bibi et al., 2016). Studies by reported a wide range of

Quick Response Code	Access this article online	
	Website: www.contaminantsreviews.com	DOI: 10.26480/ecr.02.2023.105.115

Cite The Article: Sharafa S.B., Aliyu R., Ibrahim B.B., Akpootu D.O., Tijjani B.I., Darma T.H., Ayedun F. and Sulu H.T. (2023). Analysis Of Aerosols in West Africa: Modelling and Radiative Forcing. *Environmental Contaminants Reviews, 6(2): 105-115*.

aerosol loading over various AERONET sites in West Africa during 2003–2005 (Ogunjobi et al., 2008). Recently, a group researchers reported significant heating within the atmosphere due to absorbing aerosols over selected AERONET sites in South Africa (Adesina et al., 2016; Kumar et al., 2014). In other related studies, reported invariant values of ARF over three AERONET sites in Kenya using the Coupled Ocean and Atmosphere Radiative Transfer (COART) model (Makokha et al., 2015).

It is, therefore, important we obtain accurate and detailed information on ARF over different regions of the globe, particularly least studied ones such as West Africa. Despite the reasonable amount of ground-based AERONET and satellite-based MODIS (Moderate resolution imaging spectroradiometer) data, West Africa suffers from insufficient characterization of aerosols and its radiative properties with broad consequences on its inability to quantify ARF precisely. Previous studies over the region indicated existence of fine- and coarse-mode aerosols from various natural and anthropogenic sources resulting in varying concentrations at different spatio-temporal scales (Tantre, 2003; Hatzianastassiou et al., 2004; Yu, 2006; Ogunjobi and OK, 2007; Raut and Chazette, 2007; Garcia et al., 2012). However, fundamental knowledge of key aerosol types (e.g., desert dust, biomass burning, and urban-industrial) and their modification processes, which are important in reducing uncertainties in ARF estimates is largely unknown (Annex III: Glossary In: Climate Change, 2013). Also, investigation of some key aerosol optical and radiative properties which are crucial in reducing uncertainties in ARF is nonexistent (Patel et al., 2017; Bibi et al., 2017; Tiwari et al., 2016).

In view of the immense local and regional importance of aerosols, the present study seeks to investigate the aerosol optical, microphysical and radiative properties over Cinzana and Ilorin, two tropical sites located in West Africa. The study utilized 15 years (February, 2000 to July, 2015) of Level 2.0 (high quality cloud-screened and quality assured) data of some aerosol properties derived from MODIS satellite to examine (i) the time series modeling and prediction of aerosol optical depth (AOD, τ), Ångström exponent (AE, α), cloud fraction (N_{cloud}) and single scattering albedo (SSA, ω_o), (ii) their temporal variability and distributions, and (iii) the shortwave radiation budget.

1.1 Related Literatures

There has been limited model-observation comparison studies. For the places where this has been done, there has been mismatch biases of either positive or negative values (Pan, 2019; Dasari, 2020). The results from the validation of the modeled data with the measured data show good agreement with low values of error parameters in the sub-Saharan African region for AOD and AE (Sharafa, 2020). The seasonal aerosol radiative forcing efficiency (ARFE) in the atmosphere of Dushanbe, Tajikistan was found high (>100 Wm^{-2}) and consistent throughout the year. Consequently, this resulted in similar seasonally coherent high atmospheric solar heating rate (HR) during all seasons. High ARFE and HR values are indication that the atmospheric aerosols could exert significant implications to regional air quality, climate and cryosphere over the central Asian region and downwind Tianshan and Himalaya-Tibetan Plateau mountain regions with sensitive ecosystems (Rupakheti et al., 2020). The aerosols over the Pokhara Valley, a site in the Himalayan foothills were able to exert regionally coherent radiative forcing and atmospheric heating, making aerosols as a major driver of climate change in the region and broader surrounding regions. Also, the analysis on all the key aerosol parameters and their radiative effects covering a large spatial domain on a seasonal scale can be used as inputs in global climate models to assess and predict the anthropogenic effects of aerosol forcing on climate and climate change over an aerosol hotspot (Ramachandran and Rupakheti, 2020)

2. Materials and Methods

2.1 Data Collection

The West African region is associated with a marked seasonal cycle. From November to February most of the region is dominated by dry north-easterly winds from the Sahara. Clouds and precipitation are confined to the coastal strip, where the sea-breeze circulation brings in moister air. Large amounts of mineral dust from the Sahel and Sahara are transported across the region, which in combination with human-induced biomass burning lead to persistent haze because of the lack of wet removal. From March onwards the south-westerly winds begin to penetrate deeper into the continent, bringing with them moister air, more clouds and precipitation (Sultan and Janicot, 2003). The wind retreats back to the southern parts of West Africa in September and October. The collocated data of AERONET and MODIS data used in this work were downloaded from the website of Multi-sensor Aerosol Products Sampling System (MAPSS) (http://giovanni.gsfc.nasa.gov/mapss/). This is because it provides a consistent sampling approach that enables easy and direct inter-comparison and validation of the different quality assured aerosol products from the two sensors in a uniform and consistent way (Petrenko et al., 2012). The long time-series (2000-2015) of MODIS measurements of aerosol optical depth (τ_{550}), Angsrom exponent ($\alpha_{470-660}$), cloud fraction (N_{cloud}), fine mode fraction (FMF) and single scattering albedo (ω_o) were used in this study for TS modeling and forecasting, as well as the aerosol radiative forcing (AFR) analysis on the climate over West Africa. The study covers the AERONET stations in Cinzana and Ilorin. The coordinates, altitude and raining season of the stations are shown in Table 1.

Table 1: Aeronet Stations in The Sub-Saharan Africa and Their Coordinates

S/No	Country	Aeronet station	Longitude	Latitude	Altitude	Raining season
1.	Mali	Cinzana	5°W	13°N	285 m	Apr. – Oct.
2.	Nigeria	Ilorin	4°E	8°N	350 m	Apr. – Oct.

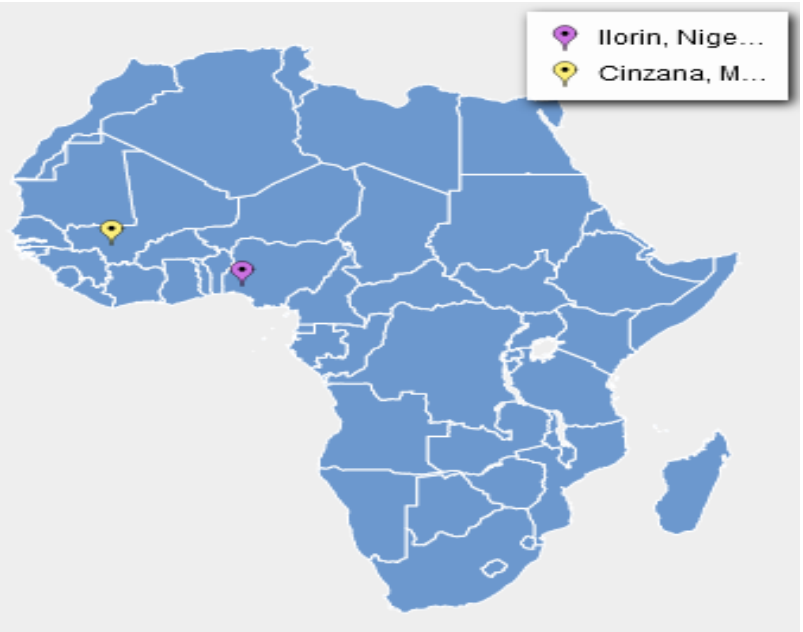

Figure 1: Map of Cinzana and Ilorin (West Africa)

Figure 1 shows the location of both Cinzana and Ilorin on the African map. The value of τ is a measure of aerosol loading. Unpolluted atmospheric conditions should have τ values between 0.04 and 0.06 (Tan et al., 2015). The value of α provides first-hand information on the aerosol size distribution trend. The α value varies from 1 to 3 for fresh and aged smoke, and urban aerosol particles, while it is nearly zero for coarse mode aerosols such as dust and sea salt (Eck, 1999). The N_{cloud} value is a measure of the amount of cloud in the atmosphere. The value of ω_o can determine the sign of the aerosol radiative effects. Pure light absorbing carbon particles typically have a ω_o value of 0.2 while its value for scattering is close to unity (Bergstrom, 2007; Moosmuller and Chakrabarty, 2011). The FMF values can vary from 0 (single coarse mode aerosol) to 1 (single fine mode aerosol), and provides quantitative information on the nature of the aerosol size distribution (Kedia et al., 2014).

2.2 Data Analysis

The aerosol optical properties data from MAPSS obtained for the study period are daily data. The large data density for the period makes it easier for monthly cycle and distribution trends of the parameters to be distinguished. The daily data were used to compute the monthly and seasonal averages over the entire period of study. The dataset were divided into raining season and dry season data. The TS model statistics and model parameters of the aerosol optical parameters for each of the study area were derived using Expert Modeler in the SPSS analysis software. The data used for the modelling phase was from the year 2000 – June 2014. The derived models were used to predict a year (July 2014 – June 2015) data for each of the parameters in each station. To evaluate the performance of the models, four groups of accuracy measures were considered: ability to predict (R^2 and stationary R^2), precision (RMSE, MAPE and MAE), goodness-of-fit (BIC) and significance (p-value). Lower values of the BIC, MAE, MAPE, RMSE and significance (p-value < 0.05) and a high value of R^2 and stationary R^2 are the standard for a good model.

Equation (1) was used for estimating the direct aerosol radiative forcing, ΔF_R at the top of the atmosphere (Chylek and Wong, 1995; Tijjani and Akpootu, 2012; Sharafa et al., 2018).

$$\Delta F_R = -\frac{S_o}{4} T_{atm}^2 (1 - N_{cloud}) 2\tau\{(1-A)^2 \beta\omega - 2A(1-\omega)\} \quad (1)$$

where S_o is the solar constant with a value of 1368 Wm^{-2}, T_{atm} is the transmittance of the atmosphere above the aerosol layer with a value of 0.79, N_{cloud} is the cloud fraction, τ is the aerosol optical depth, ω is the average single scattering albedo of the aerosol layer, A is the albedo of the underlying surface which has a value of 0.22 for land retrievals and β is the fraction of radiation scattered by aerosol into the atmosphere which was calculated from eqn. (2) (Akpootu and Momoh, 2013). The other parameters were extracted from the retrieved MODIS aerosol data.

$$\tau_{ext}(\lambda) = \beta\lambda^{-\alpha_{ext}} \quad (2)$$

where τ_{ext} is the aerosol optical depth at a reference wavelength λ, β is the Angstrom turbidity coefficient, and α_{ext} is the Angstrom exponent.

3. Results and Discussions

3.1 Time Series Analysis and Prediction

3.1.1 T_{550} Analysis and Prediction

The TS model statistics of the τ_{550} for each of the AERONET stations are given in Tables 6 - 7.

Cinzana

Table 6: Model summary of τ_{550} at Cinzana station (Mali)

Model				Simple Seasonal		
Stationary R^2	R^2	RMSE	MAPE	MAE	Normalized BIC	Sig.
0.630	0.514	0.159	30.797	0.113	-3.615	0.000
Exponential smoothing model parameters						
No Transformation			Estimates			Sig.
Alpha (Level)			0.100			0.006
Delta (Season)			8.027E-007			*1.000*

From the Table 6, the model obtained for τ_{550} values in Cinzana is simple seasonal exponential smoothing. This shows that the τ_{550} in this station did not increase significantly over the years and its seasonal effect is constant for these years. The values of the stationary R^2 (0.630) and R^2 (0.514) show that the model is good, and statistically significant. The low values of RMSE (0.159), MAPE (30.797), MAE (0.113) and a negative Normalized BIC (-3.615) shows that the model is good. Also, from the values of the significance of the model parameters, it can be seen that the level parameter is statistically significant at 95 % significance level while the season parameter is not. The season parameter indicates that the aerosol loading in this station is seasonal in nature.

Figure 2 show plots of τ_{550} values measured and predicted for Cinzana station. The plots show that the model can estimate the parameters, notwithstanding the overestimation and underestimation observed in the predicted values. None of the predicted data was perfect, but there is a significant departure between the measured and predicted data in April and June of 2015. Also, a very close value was observed in October and November of 2014.

From the Table 7, the model obtained for τ_{550} values in Ilorin is simple seasonal exponential smoothing. This shows that the τ_{550} in this station did not increase significantly over the years and its seasonal effect is constant for these years. The values of the stationary R^2 (0.773) and R^2 (0.637) show that the model is good, but statistically insignificant. The low values of RMSE (0.229), MAPE (27.478), MAE (0.170) and a negative Normalized BIC (-2.879) shows that the model is good. Also, from the values of the significance of the model parameters, it can be seen that the level parameter is statistically significant at 95 % significance level while the season parameter is not. The season parameter indicates that the aerosol loading in this station is seasonal in nature.

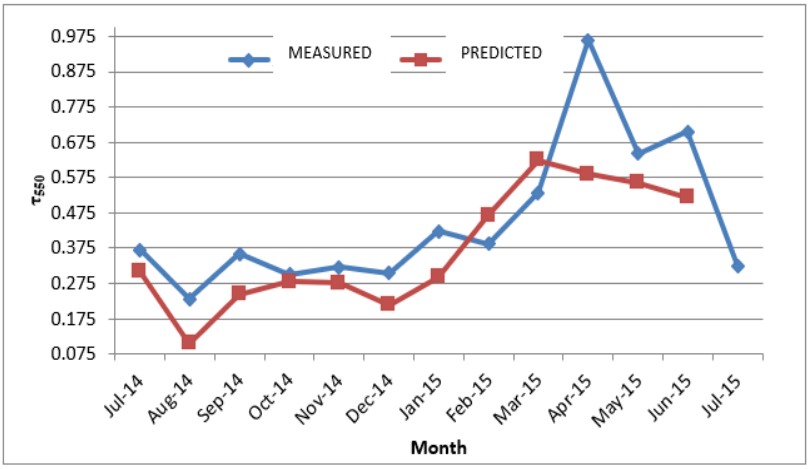

Figure 2: The plots of measured and predicted τ_{550} for Cinzana station using time series analysis

Table 7: Model summary of τ_{550} at Ilorin station (Nigeria)						
Model				Simple Seasonal		
Stationary R^2	R^2	RMSE	MAPE	MAE	Normalized BIC	Sig.
0.773	0.637	0.229	27.478	0.170	-2.879	0.093
Exponential smoothing model parameters						
No Transformation			Estimates			Sig.
Alpha (Level)			0.100			0.041
Delta (Season)			3.035E-006			*1.000*

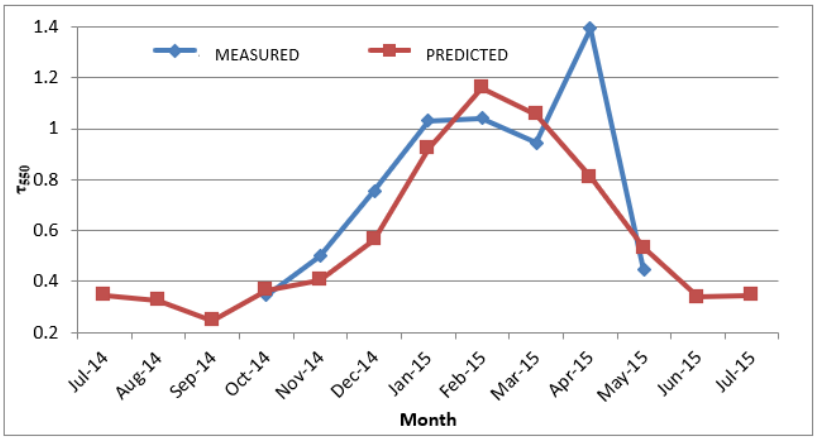

Figure 3: The plots of measured and predicted τ_{550} for Ilorin station using time series analysis

Figure 3 show plots of τ_{550} values measured and predicted for Ilorin station. The plots show that the model can estimate the parameters, notwithstanding the overestimation and underestimation observed in the predicted values. Five months measured data (July 2014, August 2014, September 2014, June 2015 and July 2015) were missing; only the predicted data for October 2014 was perfect.

3.1.2 $\alpha_{470\text{-}660}$ Analysis and Prediction

The TS model statistics of the $\alpha_{470\text{-}660}$ values for each of the AERONET stations are given in Tables 8 – 9.

From the Table 8, the model obtained for the $\alpha_{470\text{-}660}$ *values* at Cinzana is simple seasonal exponential smoothing. This shows that the $\alpha_{470\text{-}660}$ values in this station did not increase over the years and its seasonal effect is constant for these years. The values of the stationary R^2 (0.730) and R^2 (0.591) show that the model is good, and also statistically significant. The low values of RMSE (0.231), MAPE (84.744), MAE (0.177) and a negative Normalized BIC (-2.869) shows that the model is good. Also, from the values of the significance of the model parameters, it can be seen that the level parameter is statistically significant at 95 % significance level while the season parameter is not. The season parameter in this model shows that the trend is seasonal, even if not significant.

Table 8: Model Summary of $\alpha_{470\text{-}660}$ at Cinzana station (Mali)						
Model				Simple Seasonal		
Stationary R^2	R^2	RMSE	MAPE	MAE	Normalized BIC	Sig.
0.730	0.591	0.231	84.744	0.177	-2.869	0.018
Exponential smoothing model parameters						
No Transformation			Estimates			Sig.
Alpha (Level)			0.300			0.000
Delta (Season)			1.003E-005			*1.000*

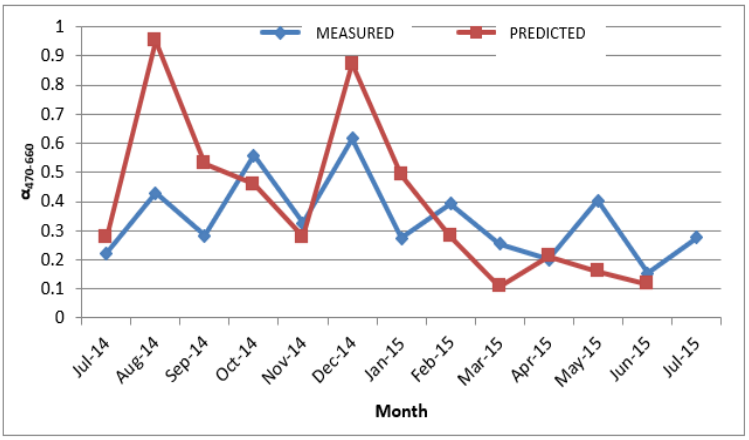

Figure 4: The plots of measured and predicted $\alpha_{470\text{-}660}$ for Cinzana station using time series analysis

Figure 4 show plots of $\alpha_{470\text{-}660}$ values measured and predicted for Cinzana station. The plots show that the model can estimate the parameters, notwithstanding the overestimation and underestimation observed in the predicted values. Only the predicted data for April 2015 was perfect.

From the Table 9, the model obtained for the $\alpha_{470\text{-}660}$ *values* at Ilorin is simple seasonal exponential smoothing. This shows that the $\alpha_{470\text{-}660}$ in this station did not increase over the years and its seasonal effect is constant for these years. The values of the stationary R^2 (0.719) and R^2 (0.502) show that the model is good, and also statistically significant. The low values of RMSE (0.308), MAPE (51.045), MAE (0.228) and a negative Normalized BIC (-2.287) shows that the model is good. Also, from the values of the significance of the model parameters, it can be seen that the level parameter is statistically significant at 95 % significance level while the season parameter is not. The season parameter in this model shows that the trend is seasonal, even if not significant.

Figure 5 show plots of $\alpha_{470\text{-}660}$ values measured and predicted for Ilorin station. The plots show that the model can estimate the parameters, notwithstanding the overestimation and underestimation observed in the predicted values. Predicted data for July 2014, September 2014 and June 2015 were perfect.

Table 9: Model summary of $\alpha_{470-660}$ at Ilorin station (Nigeria)						
Model				Simple Seasonal		
Stationary R^2	R^2	RMSE	MAPE	MAE	Normalized BIC	Sig.
0.719	0.502	0.308	51.045	0.228	-2.287	0.000
Exponential smoothing model parameters						
No Transformation			Estimates			Sig.
Alpha (Level)			0.100			0.003
Delta (Season)			5.332E-006			*1.000*

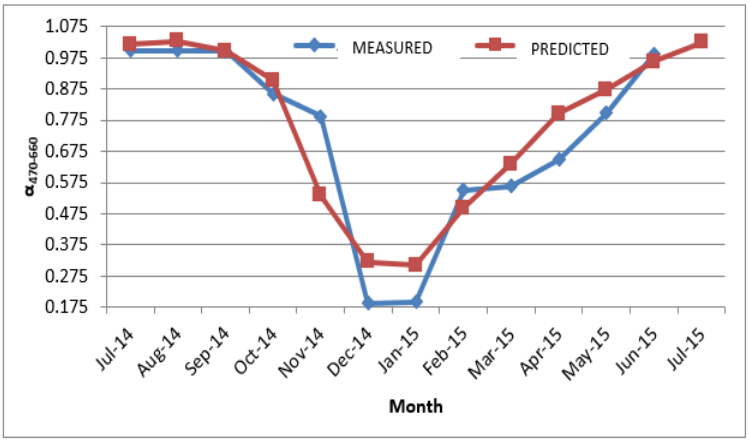

Figure 5: The plots of measured and predicted $\alpha_{470-660}$ for Ilorin station using time series analysis

3.1.3 N_{cloud} Analysis and Prediction

The TS model statistics of the N_{cloud} values for each of the AERONET stations are given in Tables 10 – 11.

From the Table 10, the model obtained in Cinzana is simple seasonal exponential smoothing. This shows that the N_{cloud} in this station did not increase significantly over the years and its seasonal effect is constant for these years. The values of the stationary R^2 (0.720) and R^2 (0.790) show that the model is good, but statistically insignificant. The low values of RMSE (0.083), MAPE (21.934), MAE (0.067) and a negative Normalized BIC (-4.927) shows that the model is good. Also, from the values of the significance of the model parameters, it can be seen that both parameters are not statistically significant at 95 % significance level. The season parameter indicates that the cloud cover in this station is seasonal in nature.

Table 10: Model Summary of N_{cloud} at Cinzana station (Mali)						
Model				Simple Seasonal		
Stationary R^2	R^2	RMSE	MAPE	MAE	Normalized BIC	Sig.
0.720	0.790	0.083	21.934	0.067	-4.927	0.451
Exponential smoothing model parameters						
No Transformation			Estimates			Sig.
Alpha (Level)			0.002			0.747
Delta (Season)			8.057E-006			*0.999*

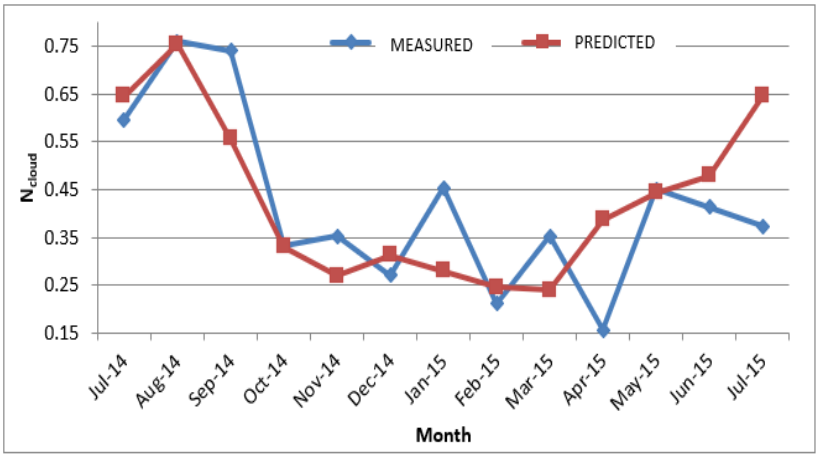

Figure 6: The plots of measured and Predicted N_{cloud} for Cinzana station using time series analysis

Figure 6 show plots of N_{cloud} values measured and predicted for Cinzana station. The plots show that the model can estimate the parameters, notwithstanding the overestimation and underestimation observed in the predicted values. Three of the predicted data were perfect, and they are august and October 2014, and May 2015.

From the Table 11, the model obtained in Ilorin is simple seasonal exponential smoothing. This shows that the N_{cloud} in this station did not increase significantly over the years and its seasonal effect is constant for these years. The values of the stationary R^2 (0.750) and R^2 (0.885) show that the model is good, and statistically significant. The low values of RMSE (0.093), MAPE (39.164), MAE (0.065) and a negative Normalized BIC (-4.655) shows that the model is good. Also, from the values of the significance of the model parameters, it can be seen that both parameters are not statistically significant at 95 % significance level. The season parameter indicates that the cloud cover in this station is seasonal in nature.

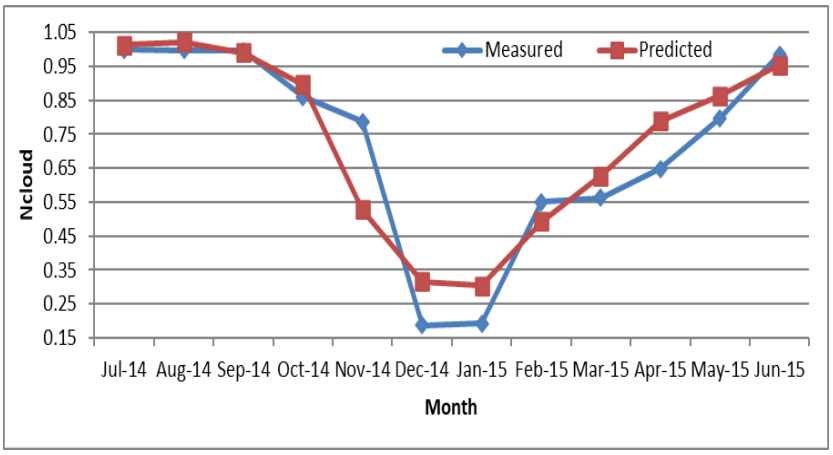

Figure 7: The plots of measured and Predicted N_{cloud} for Ilorin station using time series analysis

Figure 7 show plots of N_{cloud} values measured and predicted for Ilorin station. The plots show that the model can estimate the parameters, notwithstanding the overestimation and underestimation observed in the predicted values. Only the predicted data for July and September 2014 were perfect.

3.1.4 ω_o analysis and prediction

The TS model statistics of the ω_o values for each of the AERONET stations are given in Tables 12 – 13.

From the Table 12, the model obtained in Cinzana for ω_o values is simple seasonal exponential smoothing. This shows that the ω_o in this station did not increase significantly over the years and its seasonal effect is constant for these years. The values of the stationary R^2 (0.486) and R^2 (0.749) show that the model is good, and statistically significant. The low values of RMSE (0.009), MAPE (0.679), MAE (0.006) and a negative Normalized BIC (-9.347) shows that the model is good. Also, from the values of the significance of the model parameters, it can be seen that the level parameter is statistically significant at 95 % significance level while the season parameter is not. The season parameter indicates that the ω_o in this station is seasonal in nature.

Figure 8 show plots of ω_o values, measured and predicted for Cinzana station. The plots show that the model can estimate the parameters, notwithstanding the overestimation and underestimation observed in the predicted values. Only the predicted data for May and June 2015 were perfect.

Table 12: Model summary of ω_o at Cinzana station (Mali)

Model				Simple Seasonal		
Stationary R^2	R^2	RMSE	MAPE	MAE	Normalized BIC	Sig.
0.486	0.749	0.009	0.679	0.006	-9.347	0.003
Exponential smoothing model parameters						
No Transformation			Estimates			Sig.
Alpha (Level)			0.300			0.000
Delta (Season)			2.556E-006			*1.000*

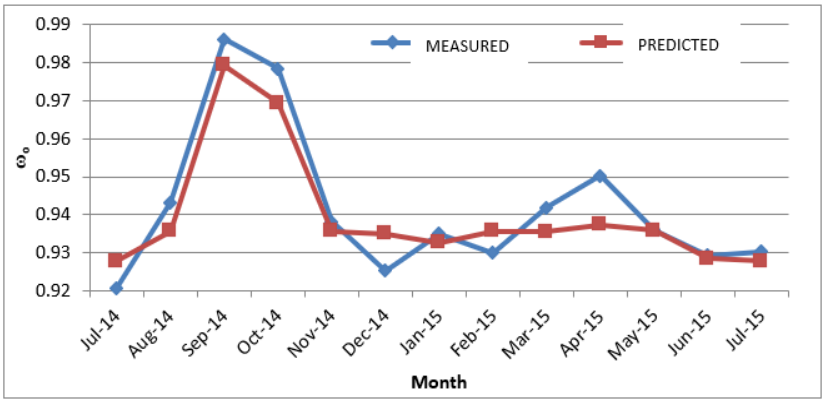

Figure 8: The plots of measured and predicted ω_o for Cinzana station using time series analysis

Table 13: Model summary of ω_o at Ilorin station (Nigeria)

Model				ARIMA (0,0,0)(0,1,1)		
Stationary R^2	R^2	RMSE	MAPE	MAE	Normalized BIC	Sig.
0.323	0.623	0.005	0.301	0.003	-10.652	0.034
Exponential smoothing model parameters						
No Transformation			Estimates			Sig.
Constant			0.000			0.033
Seasonal Difference			1			
MA Seasonal Lag 1			0.650			0.000

From the Table 13, the model obtained in Ilorin for ω_o values is ARIMA(0,0,0)(0,1,1). This model is appropriate for series with order 1 seasonal differencing and order 1 moving average and no constant. This shows that the ω_o in this station has a seasonal effect for these years. The values of the stationary R^2 (0.323) and R^2 (0.623) show that the model is good, and statistically significant. The low values of RMSE (0.005), MAPE (0.301), MAE (0.003) and a negative Normalized BIC (-10.652) shows that the model is good. Also, from the values of the significance of the model parameters, it can be seen that the constant and seasonal MA parameters are statistically significant at 95 % significance level. This also shows the

presence of seasonal features in the station.

Figure 9 show plots of ω_o values measured and predicted for Ilorin station. The plots show that the model can estimate the parameters, notwithstanding the overestimation and underestimation observed in the predicted values. Notwithstanding that five measured data that were missing, the model was able to predict three months perfectly i.e., October 2014, November 2014 and March 2015.

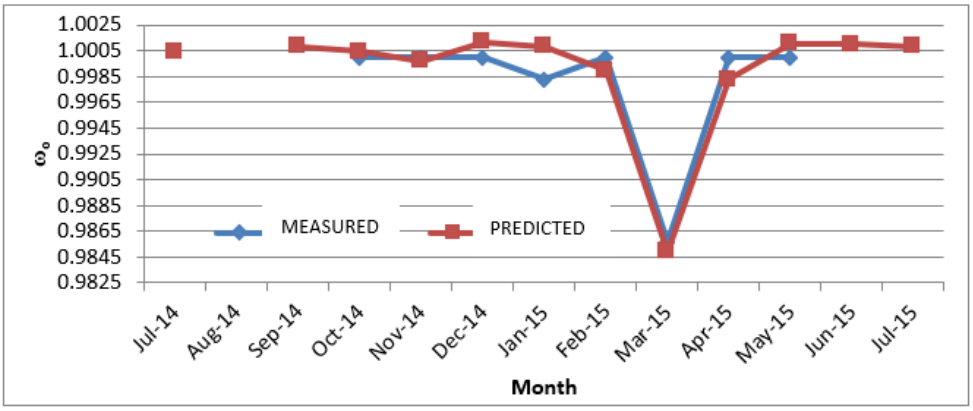

Figure 9: The plots of measured and predicted ω_o for Ilorin station using time series analysis

3.1.5 FMF Analysis and Prediction

The TS model statistics of the FMF values for each of the AERONET stations are given in Tables 14 – 15.

From the Table 14, the model obtained in Cinzana for FMF values is simple seasonal exponential smoothing. This shows that the FMF in this station did not increase significantly over the years and its seasonal effect is constant for these years. The values of the stationary R^2 (0.741) and R^2 (0.115) show that the model is good, and statistically significant. The low values of RMSE (0.067), MAPE (78.768), MAE (0.043) and a negative Normalized BIC (-5.339) shows that the model is good. Also, from the values of the significance of the model parameters, it can be seen that the level parameter is statistically significant at 95 % significance level while the season parameter is not. The season parameter indicates that the FMF in this station is seasonal in nature. There are equally some missing data in the series.

Figure 10 show plots of FMF values measured and predicted for Cinzana station. The plots show that the model cannot estimate the parameters correctly. Measured data for five months (January to May 2015) were missing and none of the predicted data was perfect.

Table 14: Model Summary of FMF at Cinzana Station (Mali)

Model				Simple Seasonal		
Stationary R^2	R^2	RMSE	MAPE	MAE	Normalized BIC	Sig.
0.741	0.115	0.067	78.768	0.043	-5.339	0.004
Exponential smoothing model parameters						
No Transformation			Estimates			Sig.
Alpha (Level)			0.100			0.011
Delta (Season)			1.727E-006			*1.000*

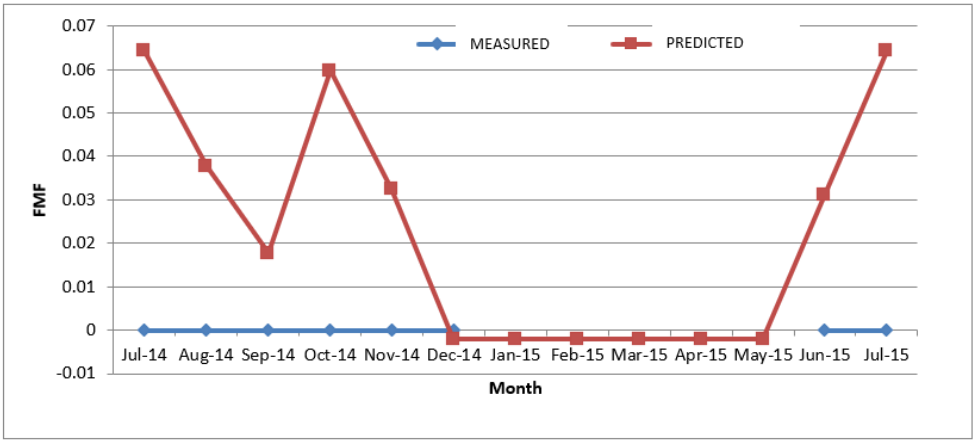

Figure 10: The plots of measured and predicted FMF for Cinzana station using time series analysis

Table 15: Model Summary of FMF at Ilorin Station (Nigeria)

Model				Simple Seasonal		
Stationary R^2	R^2	RMSE	MAPE	MAE	Normalized BIC	Sig.
0.718	0.350	0.210	60.651	0.162	-3.052	0.482
Exponential smoothing model parameters						
No Transformation			Estimates			Sig.
Alpha (Level)			0.100			0.009
Delta (Season)			0.000			*0.998*

From the Table 15, the model obtained in Ilorin for FMF values is simple seasonal exponential smoothing. This shows that the FMF in this station did not increase significantly over the years and its seasonal effect is constant for these years. The values of the stationary R^2 (0.718) and R^2 (0.350) show that the model is good, but not statistically significant. The low values of RMSE (0.210), MAPE (60.651), MAE (0.162) and a negative Normalized BIC (-3.052) shows that the model is good. Also, from the values of the significance of the model parameters, it can be seen that the

level parameter is statistically significant at 95 % significance level while the season parameter is not. The season parameter indicates that the FMF in this station is seasonal in nature. There are equally some missing data in the series.

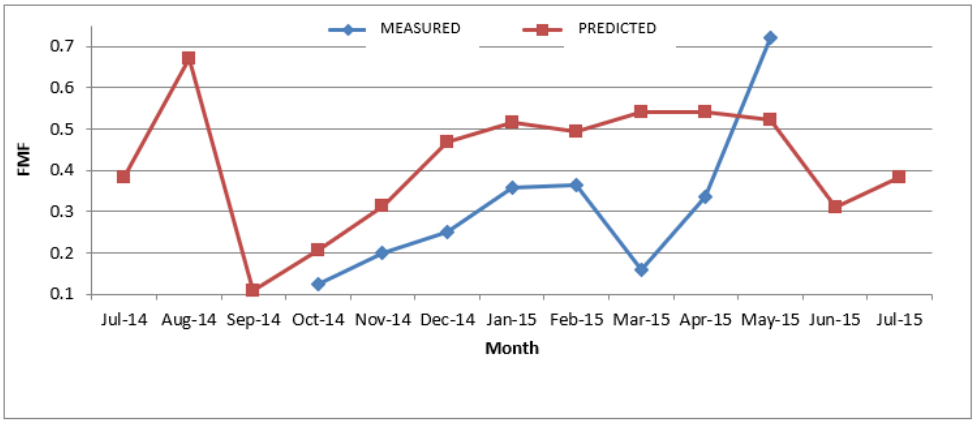

Figure 11: The Plots of Measured and Predicted FMF for Ilorin Station Using Time Series Analysis

Figure 11 show plots of FMF values measured and predicted for Ilorin station. The plots show that the model cannot estimate the parameters correctly. Five of the measured data were missing, and none of the predicted data was perfect.

3.2 Spatio-Temporal Distribution of the MODIS Aerosol Optical Depth

Figure 12 shows the seasonal cycle of the MODIS aerosol loading (τ_{550}) averaged between 2000 and 2015 for the two AERONET stations at a wavelength of 550 nm. The concentration of aerosols is strongest between January and April with the peaks of each station spread across the months. The τ_{550} is highest during February in Ilorin (1.20) and during March in Cinzana (0.67). It can be observed from the figure that the aerosol loading trend of the stations agrees with the two seasons (dry and raining). The onset of raining season in the stations is April, and the loading starts decreasing from this month up to September. This is due to the washing out of aerosols by rain. An increase in the loading is then observed from October to March, which signifies the dusty season with a peak between February and March.

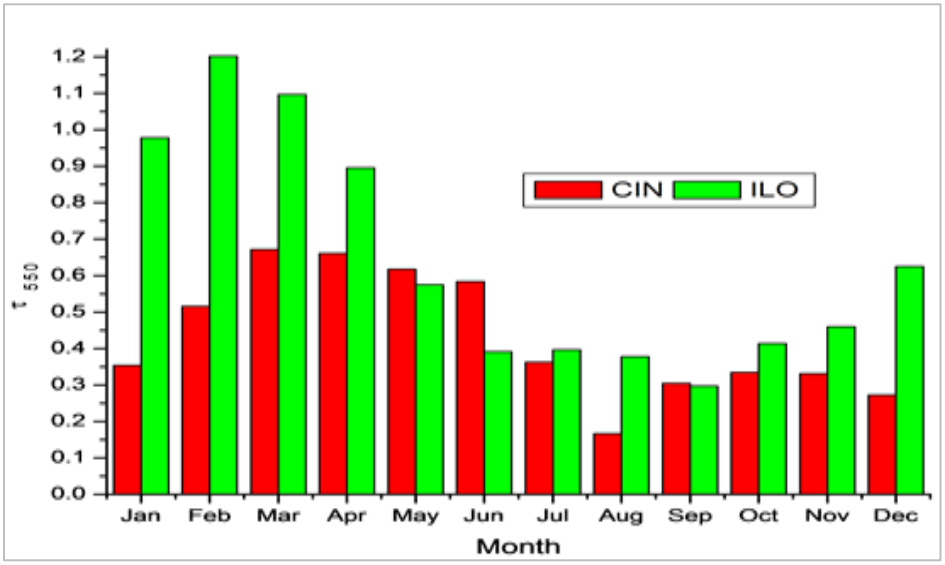

Figure 12: Histogram of the seasonal cycle of the τ_{550} over the two AERONET stations averaged between 2000 and 2015.

Table 16: The Aerosol Optical Depth (T_{550}) Averaged Between 2000 And 2015 During the Wet Season, Dry Season and Overall For The Considered AERONET Stations.

Stations	average per station	Raining season	Dry
season			
Cinzana	0.431	0.433	0.429
Ilorin	0.643	0.478	0.872

Table 16 summarizes the seasonal mean of τ_{550} for the considered AERONET stations during dry and raining seasons, averaged between 2000 and 2015. During the raining season, the station in Cinzana has a record of higher average seasonal aerosol loading values than during the dry season. This may have happened as a result of two scenarios: 1) because of delayed/short raining season, or 2) increase in usage of fossil fuel and biomass burning, or both. On the other hand, Ilorin station has a record of higher seasonal loading values during the dry season. This is as expected, because during dry season there is always a build-up of aerosols in the atmosphere. Whereas, there will be washout of aerosols during the rainy season. Ordinarily, dry season is supposed to be a season with the least humidity but the duration of raining season varies across the sub-Saharan African region. This is the reason why some stations has less loading during dry season.

3.3 Types of Particles

Figure 13 show the monthly mean MODIS $\alpha_{470\text{-}660}$ averaged between 2000 and 2015 for the two stations. The period between January and June in the West African divide is characterized by the presence of coarse (small values of $\alpha_{470\text{-}660}$) particles that are the signature of mineral dust aerosols. When considering Ilorin station, it can be observed that the station is under fine particle influence during the months of July through October, while Cinzana station seems to be under dust influence throughout the year. Similar observation was reported by Tanré *et al.* (2003). It can be observed from the figure that the aerosol size distribution trend of the two West African stations is different for the two seasons. As expected, the onset of raining season brings about an increase in the fine mode (anthropogenic) aerosols in this part of Africa while the dry season brings about an increase in the coarse mode aerosols.

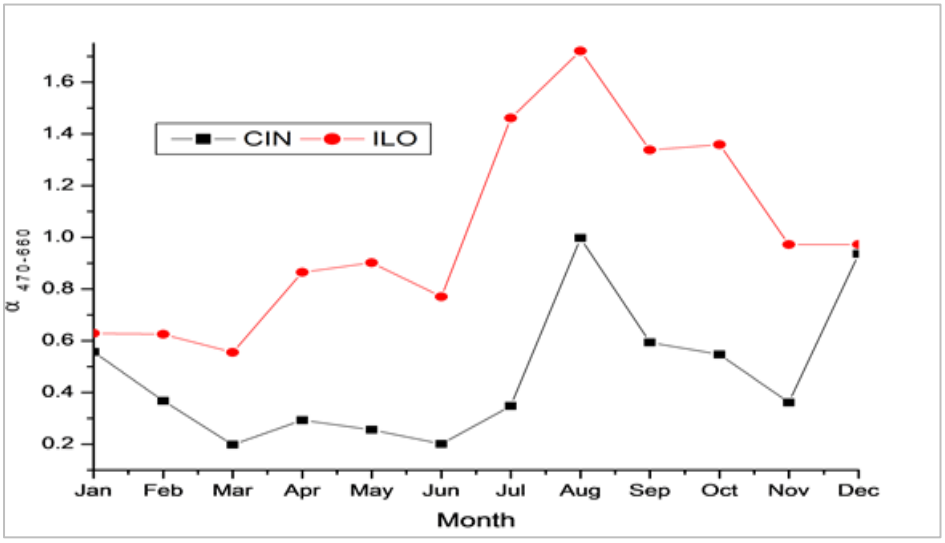

Figure 13: Seasonal cycle of $\alpha_{470\text{-}660}$ averaged between 2000 and 2015 for the two AERONET stations.

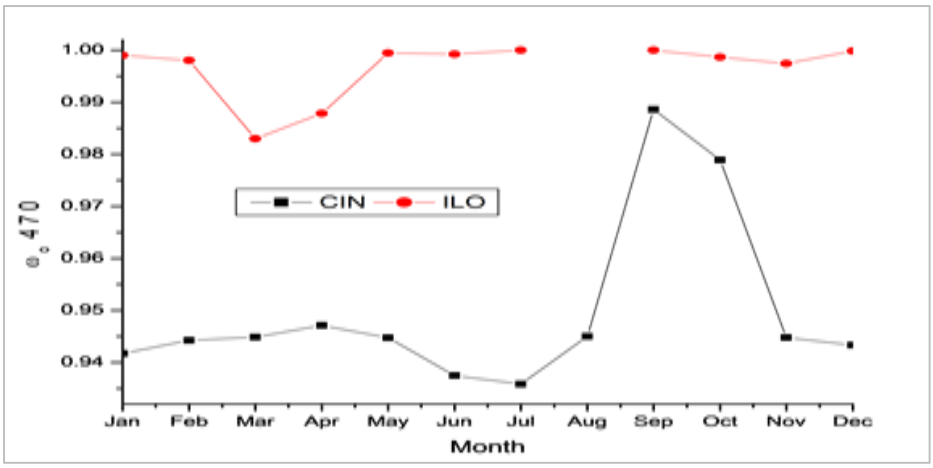

Figure 14: Seasonal cycle of the ω_o 470 averaged between 2000 and 2015 for the two AERONET stations.

Figure 14 shows the monthly mean MODIS single scattering albedo (ω_o) averaged between 2000 and 2015 for the two stations. The period between January and June in West Africa is characterized by the presence of scattering (strong values of ω_o) particles that are the signature of mineral dust aerosols. There are some episodes of fine mode aerosols in Cinzana (November to July) and Ilorin (March to April) with slightly less ω_o values. These particles correspond to a mixture of dust, urban and industrial pollution and biomass burning.

3.4 Shortwave Radiation Budget

Figure 15 present the top of the atmosphere ARF in the two stations, as estimated from eqn. (1). A general cooling trend is observed and it is due to the reflecting properties of dust particles during dry season while it is as a result of cloud during the wet season; this is called the direct aerosol effect. The maximum cooling estimated for Ilorin during February is consistent with the maximum dust loading diagnosed during the month. The highest negative forcing in Cinzana was noted in March and this is also consistent with the observed highest aerosol loading in the station. Similarly, reduction of the cooling is noted due to the decrease of dust loading (increase in α) over the two stations between the months of July and November. Warming incidents were noticed in Ilorin in the months of July to September. Maximum cooling is observed during dry season while the cooling is reduced during raining season.

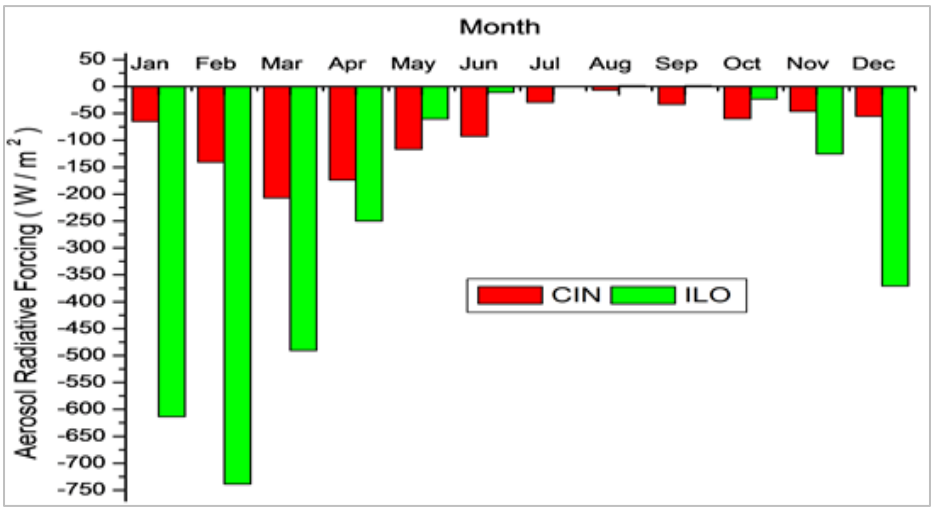

Figure 15: Histogram of the radiative forcing at the top of the atmosphere averaged between 2000 and 2015.

Table 17: Radiative forcing at the top of the atmosphere for the AERONET Stations Averaged Between 2000 And 2015 During Dry Season, Wet Season Seasons and Overall Data.

Stations	average per station (W/m^2)	Wet season (W/m^2)	Dry season (W/m^2)
Cinzana	-86.810	-74.265	-104.569
Ilorin	-262.606	-66.444	-471.507

Table 17 summarizes the mean radiative forcing estimated for the two stations, dry season and wet season. The negative forcing (cooling) is higher during the dry season for Ilorin stations; while the cooling is stronger during wet season in Cinzana station. Comparing tables 16 and 17 shows that there is a direct relationship between ARF and τ_{550} in the two stations. Also, comparing figure 10 with table 17 shows an inverse relationship between ARF and $\alpha_{470\text{-}660}$ over the study period. The two observations shows that (1) the higher the τ_{550} (aerosol loading), the higher the cooling effect on the atmosphere, and (2) the higher the $\alpha_{470\text{-}660}$ (fine mode particles), the lower the cooling effect on the atmosphere. The results also indicated that anthropogenic aerosols are mostly responsible for the reduction in the negative ARF in the study area.

4. Conclusions

Studies of modelling and AFR analysis of aerosols' parameters in West Africa are very rare. Here, we took advantage of AERONET stations ideally located in two countries in the region to explain the underlying modes and effects of the parameters on this region. This study is an attempt to link the seasonal dynamics of the atmosphere and the aerosol parameters in this region, and it also provides explanation for the aerosol deposition patterns. We have studied the seasonal variability of the distribution of desert aerosols in western Africa from their optical and physical properties. MODIS observations allowed us to show the predominant presence of Saharan dust in the atmosphere almost throughout the year. TS model equations were derived from the Expert modeler for each parameter from the two AERONET stations. All the eight models generated are exponential smoothing models, except for only ω_o in Ilorin station that has an ARIMA model.

The predicted data fairly represent the measured data in all cases considered. That is, the model was able to successfully reproduce the temporal trends of the aerosol parameters over the stations. This means that the forecasted parameters is good, and can be used for further studies in the stations. Examination of the variability of aerosol loading at each station shows that the two stations had large τ_{550} values, on average, and are dominated by desert dust. The monthly averaged τ maxima were recorded during the dry season. These indicate the prevalence of dust aerosols during the period. MODIS data also show that higher τ_{550} values associated with a lower $\alpha_{470\text{-}660}$ and higher values of ω_o were recorded from March to September showing the presence of a high concentration of coarse particles (mineral dust, sea salt). The raining season is characterized by the presence of mixtures (dust and biomass burning aerosols) of aerosol types and mostly larger values of $\alpha_{470\text{-}660}$.

The seasonal cycle of the aerosol size parameter in the region shows that most particles have large sizes i.e., mineral dust. Variation of ω_o showed that the atmosphere in the region was more of a reflecting one than absorbing, though some relatively absorbing episodes occur intermittently. Aerosol radiative forcing (ARF) at the top of the atmosphere calculated from eqn. (12) showed a general cooling trend over the two stations. The negative shortwave ARF (cooling) is stronger during the dust (dry) season. During this period, the mean value of the negative ARF is higher in Ilorin during dry season while it is higher in Cinzana during raining season. A decrease in the cooling trend tends to coincide with a decrease in dust concentration and an increase in fossil fuel usage and biomass burning. This means that for the stations considered, there is a natural shield against climate warming. Also, care must be taken in ensuring that absorbing aerosols' influences do not increase in the stations. Future field campaign experiments should provide further insight into the processes that led to the results of the AFR analysis. A tailored approach to the analysis of aerosols' diurnal cycle is needed to make the role of local circulation of aerosols in this region more apparent.

Acknowledgements

We wish to thank the Principal Investigators (PIs) of AERONET sites and their staff for establishing and maintaining these sites. In addition, I would also like to thank the Giovanni team for developing and hosting the MAPSS database and the Web MAPSS user interface.

References

2013: Annex III: Glossary In: Climate Change 2013: [Planton, S. (ed.)], IPCC, "The Physical Science Basis. Contribution of Working Group I to the Fifth Assessment Report of the Intergovernmental Panel on Climate Change [Stocker, T.F., D. Qin, G.-K. Plattner, M. Tignor, S.K. Allen, J. Boschung, A. Nauels, Y. Xia, V. Bex and P.M. Midg," 2013.

Adesina, A.J., Kumar, K.R., Sivakumar, V., and Griffith, D., 2014. Direct radiative forcing of urban aerosols over Pretoria (25.75°S, 28.28°E) using AERONET Sunphotometer data: First scientific results and environmental impact. J. Environ. Sci. (China), 26 (12).

Adesina, A.J., Kumar, R.B., Sivakumar, V., and Piketh, S.J., 2016. Intercomparison and assessment of long-term (2004–2013) multiple satellite aerosol products over two contrasting sites in South Africa. J. Atmos. Solar-Terrestrial Phys., 148, Pp. 82–95.

Akpootu, D.O., and Momoh, M., 2013. The Ångströ;m Exponent and Turbidity of Soot Component in the Radiative Forcing of Urban Aerosols. Niger. J. Basic Appl. Sci., 21 (1), Pp. 70–78.

Alam, K., Qureshi, S., and Blaschke, T., 2011. Monitoring spatio-temporal aerosol patterns over Pakistan based on MODIS, TOMS and MISR satellite data and a HYSPLIT model. Atmos. Environ., 45 (27), Pp. 4641–4651.

Alam, K., Trautmann, T., and T. Blaschke, 2011. Aerosol optical properties and radiative forcing over mega-city Karachi. Atmos. Res., 101 (3), Pp. 773–782.

Alam, K., Trautmann, T., Blaschke, T., and Majid, H., 2012. Aerosol optical and radiative properties during summer and winter seasons over Lahore and Karachi. Atmos. Environ., 50, Pp. 234–245.

Bergstrom, R.W., 2007. Spectral absorption properties of atmospheric aerosols. Atmos. Chem. Phys., 7, Pp. 5937–5943.

Bibi, H., Alam, K., Blaschke, T., Bibi, S., and Iqbal, M.J., 2016. Long-term (2007–2013) analysis of aerosol optical properties over four locations in the Indo-Gangetic plains. Appl. Opt., 55 (23).

Bibi, S., Alam, K., Chishtie, F., and Bibi, H., 2017. Characterization of absorbing aerosol types using ground and satellites-based observations over an urban environment. Atmos. Environ., 150.

Boiyo, R., Kumar, K.R., Zhao, T., and Bao, Y., 2017. Climatological analysis of aerosol optical properties over East Africa observed from space-borne sensors during 2001–2015. Atmos. Environ., 152.

Charlson, H.D.J., Schwartz, R.J., Hales, S.E., Cess, J.M., Coarkley, R.D., Jr., Hansen J.E., 1992. Climate Forcing by Anthropogenic Aerosols. Sci. New Ser., 255 (5043), Pp. 423–430.

Chylek, P., and Wong, J., 1995. Effect of absorbing aerosols on global radiation budget. Geophys. Res. Lett., 22 (8), Pp. 929–931.

Dasari, S., 2020. Source Quantification of South Asian Black Carbon Aerosols with Isotopes and Modeling. Environ. Sci. Technol.,

Eck, T.F., 1999. Wavelength dependence of the optical depth of biomass burning, urban, and desert dust aerosols. J. Geophys. Res. D Atmos., 104 (1), Pp. 31,333-31,349.

Garcia, R.D., Cachorro, V.E., Cuevas, E., Redondas, A., de Frutos, A.M., and Berjon, A., 2012. Comparison of measured and modeled UV spectral irradiance at the Izana station based on libradtran and UVA-GOA models. Opt. Pura y Apl., 45 (1), Pp. 11–15.

Hatzianastassiou, N., Katsoulis, B., and Vardavas, I., 2004. Global distribution of aerosol direct radiative forcing in the ultraviolet and visible arising under clear skies. TELLUS, 56B, Pp. 51–71.

Holben, B.Y., 1998. AERONET-A Federated Instrument Network and Data Archive for Aerosol Characterization. Remote Sens. Environ., 66, Pp. 1–16.

Kalluri, R.O.R., 2016. Direct radiative forcing properties of atmospheric aerosols over semi-arid region, Anantapur in India. Sci. Total

Environ., Pp. 566–567.

Kang, N., Kumar, K.R., Hu, K., Yu, X., and Yin, Y., 2016. Long-term (2002-2014) evolution and trend in Collection 5.1 Level-2 aerosol products derived from the MODIS and MISR sensors over the Chinese Yangtze River Delta. Atmos. Res., 181, Pp. 29–43.

Kedia, S., Ramachandran, S., Holben, B.N., and Tripathi, S.N., 2014. Quantification of aerosol type, and sources of aerosols over the Indo-Gangetic Plain. Atmos. Environ., 98, Pp. 607–619.

Kinne, S., 2003. Monthly averages of aerosol properties: A global comparison among models, satellite data, and AERONET ground data. J. Geophys. Res. Atmos., 108 (20).

Kumar, 2014. Long-term (2003-2013) climatological trends and variations in aerosol optical parameters retrieved from MODIS over three stations in South Africa. Atmos. Environ., 95, Pp. 400–408.

Kumar, K.R., 2015. Aerosol climatology and discrimination of aerosol types retrieved from MODIS, MISR and OMI over Durban (29.88°S, 31.02°E), South Africa. Atmos. Environ., 117, Pp. 9–18.

Kumar, K.R., Sivakumar, V., Reddy, R.R., Gopal, K.R., and Adesina, A.J., 2014. Identification and Classification of Different Aerosol Types over a Subtropical Rural Site in Mpumalanga, South Africa: Seasonal Variations as Retrieved from the AERONET Sunphotometer. Aerosol Air Qual. Res., 14, Pp. 108–123.

Kumar, S., Dey, S., and Srivastava, A., 2016. Quantifying enhancement in aerosol radiative forcing during 'extreme aerosol days' in summer at Delhi National Capital Region, India. Sci. Total Environ., 550, Pp. 994–1000.

Makokha, J.W., Angeyo, H.K., and Muthama, J.N., 2015. Sun-Photometric study and multivariate analysis of aerosol optical depth variability over some representative sites of the Kenyan atmosphere. Int. J. Biochem., 23, Pp. 15–28.

Moosmuller, H., and Chakrabarty, R.K., 2011. Technical Note : Simple analytical relationships between Ångström coefficients of aerosol extinction, scattering, absorption and single scattering albedo. Atmos. Chem. Phys., 11, Pp. 10677–10680.

More, S., Kumar, P.P., Gupta, P., Devara, P.C.S., and Aher, G.R., 2013. Comparison of aerosol products retrieved from AERONET, MICROTOPS and MODIS over a tropical urban city, Pune, India. Aerosol Air Qual. Res., 13 (1), Pp. 107–121.

Ogunjobi, K., Ajayi, V., Balogun, I., Omotosho, J., and He, Z., 2008. The synoptic and optical characteristics of the harmattan dust spells over Nigeria. Theor. Appl. Climatol., 93 (1–2), Pp. 91–105.

Ogunjobi, K.O., and O.K. O., 2007. Variability of Column-Integrated Aerosol Turbidity and Radiative Parameters in Sub-Saharan West Africa. Res. J. Appl. Sci., 2 (4), Pp. 505–511.

Pan, X., 2019. Six Global Biomass Burning Emission Datasets: Inter-comparison and Application in one Global Aerosol Model. Atmos. Chem. Phys. Discuss., Pp. 1–39.

Patel, P.N., Dumka, U.C., Kaskaoutis, D.G., Babu, K.N., and A.K. Mathur, 2017. Optical and radiative properties of aerosols over Desalpar, a remote site in western India: Source identification, modification processes and aerosol type discrimination. Sci. Total Environ., 575.

Petrenko, M., Ichoku, C., and Leptoukh, G., 2012. Multi-sensor Aerosol Products Sampling System (MAPSS). Atmos. Meas. Tech., 5 (5), Pp. 913–926.

Ramachandran, S., and Rupakheti, M., 2020. Inter-annual and seasonal variations in columnar aerosol characteristics and radiative effects over the Pokhara Valley in the Himalayan foothills – Composition, radiative forcing, and atmospheric heating. Environ. Pollut., 264, Pp. 1–14.

Ramanathan, V., Crutzen, P.J., Kiehl, J.T., and Rosenfeld, D., 2001. Aerosols, Climate, and the Hydrological Cycle. Sci. Compass Rev. Atmos., 294, Pp. 2119–2124.

Raut, J.C., and Chazette, P., 2007. Retrieval of aerosol complex refractive index from a synergy between lidar, sunphotometer and in situ measurements during LISAIR experiment. Atmos. Chem. Phys., 7, Pp. 2797–2815.

Remer, L.A., 2005. The MODIS Aerosol Algorithm, Products, and Validation. J. Atmos. Sci., 62 (4), Pp. 947–973.

Rupakheti, D., Rupakheti, M., Abdullaev, S.F., Yin, X., and Kang, S., 2020. Columnar aerosol properties and radiative effects over Dushanbe, Tajikistan in Central Asia. Environ. Pollut., 265, Pp. 114872.

Sharafa, S.B., 2020. Model Prediction and Climatology of Aerosol Optical Depth (τ 550) and Angstrom Exponent (α 470-660) over Three Aerosol Robotic Network Stations in sub-Saharan Africa using Moderate Resolution Imaging Spectroradiometer Data. Niger. J. Technol., 39 (1), Pp. 255–268.

Sharafa, S.B., Tijjani, B.I., Ibrahim, B.B., Sulu, H.T., Salawu, M.A., and Shehu, S.J., 2018. Seasonal variability of Aerosols and their radiative impacts on Sub-Saharan African climate during the period 2000-2015 using Modis data. Monogr. Atmos. Res. Ed. by A. B. Rabiu E. O. Abiye, Cent. Atmos. Res. Anyigba, Pp. 57–64.

Sultan, B., and Janicot, S., 2003. The West African Monsoon Dynamics. Part II: The '"Preonset"' and '"Onset"' of the Summer Monsoon. J. Clim., 16, Pp. 3407–3427.

Tan, F., Lim, H.S., Abdullah, K., Yoon, T.L., and Holben, B., 2015. Monsoonal variations in aerosol optical properties and estimation of aerosol optical depth using ground-based meteorological and air quality data in Peninsular Malaysia. Atmos. Chem. Phys., 15 (7).

Tanré, D., 2003. Measurement and modeling of the Saharan dust radiative impact: Overview of the Saharan Dust Experiment (SHADE). J. Geophys. Res., 108 (D18), Pp. 8574.

Tijjani, B.I., and Akpootu, D.O., 2012. The effect of Soot and Water Solubles in Radiative Forcing of Urban Aerosols. Int. J. Res. Rev. Pharm. Appl. Sci., 2 (6), Pp. 1128–1143.

Tiwari, S., Mishra, A.K., and Singh, A.K., 2016. Aerosol climatology over the Bay of Bengal and Arabian Sea inferred from space-borne radiometers and lidar observations. Aerosol Air Qual. Res., 16 (11), Pp. 2855–2868.

Yu, H., 2006. A review of measurement-based assessments of the aerosol direct radiative effect and forcing. Atmos. Chem. Phys., 6, Pp. 613–666.

Zhang, J., and Reid, J.S., 2010. A decadal regional and global trend analysis of the aerosol optical depth using a data-assimilation grade over-water MODIS and Level 2 MISR aerosol products. Atmos. Chem. Phys., 10 (22), Pp. 10949–10963.

Zheng, Y., 2016. A 20-year simulated climatology of global dust aerosol deposition. Sci. Total Environ., 557–558, Pp. 861–868.